Available online at www.sciencedirect.com
SCIENCE DIRECT
Journal of Solid State Chemistry 179 (2006) 1808–1813
JOURNAL OF SOLID STATE CHEMISTRY
www.elsevier.com/locate/jssc

Crystal structure, magnetic susceptibility and Mössbauer spectroscopy of the mixed-valence iron phosphate $Na_{1/2}Cu_{4/3}Fe_2(PO_4)_3$

Mourad Hidouri[a], Besma Lajmi[a], Alain Wattiaux[b], Léopold Fournés[b], Jacques Darriet[b], Mongi B. Amara[a,*]

[a]*Laboratoire de Chimie Structurale des Matériaux, Département de Chimie, Faculté des Sciences, 5019 Monastir, Tunisia*
[b]*Institut de Chimie de la Matière Condensée de Bordeaux, CNRS, 87, Avenue du Dr. A. Schweitzer, 33608 Pessac-Cedex, France*

Received 17 December 2005; received in revised form 17 March 2006; accepted 19 March 2006
Available online 24 April 2006

Abstract

Single crystals of a new mixed-valent iron phosphate $Na_{1/2}Cu_{4/3}Fe_2(PO_4)_3$ have been synthesized by a flux method and structurally characterized from X-ray diffraction data. Crystal data: space group $P\bar{1}$; $a = 6.2882(1)$ Å; $b = 8.0459(1)$ Å; $c = 9.3255(1)$ Å; $\alpha = 105.881(1)^\circ$; $\beta = 107.202(1)^\circ$; $\gamma = 101.467(1)^\circ$; $Z = 2$; $R_1 = 0.03$; w$R_2 = 0.093$. The three-dimensional structure was found to be closely related to that of the well known Howardevansite structural type. It results from infinite chains of CuO_5 and FeO_6 polyhedra, joined together by $(Cu,\square)O_6$ octahedra and PO_4 tetrahedra by corner-sharing. The large cavities in framework are occupied by Na^+ ions. The magnetic susceptibility study revealed an antiferromagnetic behavior with Neel temperature of approximately 40 K. The Mössbauer spectroscopy confirmed the presence of iron in both +2 and +3 oxidation states.

Keywords: Phosphate; X-ray diffraction; Howardevansite; Magnetic measurements; Mössbauer spectroscopy

1. Introduction

Our recent investigation of iron monophosphates belonging to the A_3PO_4–$M_3(PO_4)_2$–$FePO_4$ with A and M are an alkali metal and a divalent cations, respectively, have led to synthesis of several compounds using either a flux method or a solid state reaction techniques [1–8]. The structures of the synthesized compounds consists of bi- or three-dimensional frameworks, in which iron can adopt various environment polyhedra: tetrahedron [2,5], trigonal bipyramid [3,5] or octahedron [1,5,8]. These polyhedra are connected together either directly, by corner or edge-sharing [3,7] or via the corners or edges of the M polyhedra and the phosphate tetrahedra. The resulting frameworks usually contain cavities or tunnels where the A cations are located.

In the present paper, we report the crystallization and structural characterization, by X-ray diffraction, magnetic susceptibility and Mössbauer spectroscopy of a mixed-valent iron monophosphate with a $Na_{1/2}Cu_{4/3}Fe_2(PO_4)_3$ chemical formula. Its structure is closely related to that of the mineral Howardevansite $NaCuFe_2(VO_4)_3$ [9]. However, these compounds are not isostructural since the distribution of the Cu and Na cations is not the same.

2. Experimental section

2.1. Synthesis

Crystals of the title compound were obtained during an attempt to grow iron monophosphates by a flux method. A mixture of 12.24 g of $Fe(NO_3)_3 \cdot 9H_2O$ + 2.46 g of $Cu(NO_3)_2 \cdot 3H_2O$ + 4.02 g of $(NH_4)_2HPO_4$ + 1.07 g of Na_2CO_3 + 2.90 g of MoO_3 was ground, placed in a platinum crucible and then subjected to the following treatment: Firstly, the mixture was heated up to 673 K for 24 h to decompose H_2O, NH_3 and CO_2. Secondly, it was melted at 1173 K for 1 h and then cooled slowly at 10 K h^{-1} rate to 673 K. The furnace was then allowed to cool to room

*Corresponding author. Fax: +216 73 500 278.
E-mail address: Mongi.Benamara@fsm.rnu.tn (M.B. Amara).

0022-4596/$ - see front matter © 2006 Elsevier Inc. All rights reserved.
doi:10.1016/j.jssc.2006.03.025

temperature without control. Finally, the product was washed by warm water to dissolve the $Na_2Mo_2O_7$ flux.

2.2. Structure determination

A brown single crystal with dimensions $0.1 \times 0.1 \times 0.15\,mm^3$ was selected for the structure determination. The main experimental data collection, crystallographic data and conditions for structure resolution and refinements are listed in Table 1. Data were collected by a Kappa CCD area detector diffractometer using a graphite monochromated Mo$K\alpha$ radiation ($\lambda = 0.71073$ Å). A total of 14707 intensity reflexions were collected in the range $2.45 \leqslant \theta \leqslant 30.04$. Unit cell dimensions were determined by refinement of 2369 peak positions having $0.99 \leqslant \theta \leqslant 30.04$. Data merging ($R_{int} = 0.054$) resulted in 2405 unique reflections, of which 2245 were considered as observed [$F_o^2 > 4\sigma(F_o^2)$]. Corrections were made for Lorentz and polarization effects and absorption (transmission factors: 0.37–0.50). Based on statistical analysis of intensity distribution and successful solution of the structure, the space group was determined to be $P\bar{1}$ (no. 2). Direct methods (SIR-92) [10] were used to locate the Cu and Fe atoms and the remaining atom positions were found from successive difference Fourier maps. Refinements were made on F_o^2 using SHELXL97 [11]. All atoms were refined with anisotropic thermal parameters, resulting in the final reliability factors: $R_1 = 0.03$ and $wR_2 = 0.093$ for the observed reflections. Atomic coordinates and isotropic thermal parameters are given in Table 2. Selected bond distances and angles are listed in Table 3.

Table 1
Crystallographic data for $Na_{1/2}Cu_{4/3}Fe_2(PO_4)_3$

Crystal data	
Chemical formula	$Na_{1/2}Cu_{4/3}Fe_2(PO_4)_3$
Formula weight/g mol^{-1}	483.14
Cell setting	Triclinic
Space group	$P\bar{1}$
Cell dimensions/Å, °	$A = 6.2882(1)$
	$B = 8.0459(1)$
	$C = 9.3255(1)$
	$\alpha = 105.881(1)$
	$\beta = 107.202(1)$
	$\gamma = 101.467(1)$
Volume (Å^3)	412.52(1)
Z	2
Dc/g cm^{-3}	3.89
Data collection	
Diffractometer	Kappa CCD
λ/Å	Mo$K\alpha$/0.71073
μ /mm^{-1}	6.73
θ/°	2.45–30.04
Unique reflections/R_{int}	2405/0.0543
Observed reflections	2245
Criterion for observed reflections	[$F_o > 4\sigma(F_o)$]
Indices	$-8 \leqslant h \leqslant 8$, $-11 \leqslant k \leqslant 11$, $-13 \leqslant l \leqslant 13$
F(000)	466.0
Refinement	
Intensity correction	Lorentz-polarization
Resolution method	Direct method
Final R indices	$R_1 = 0.03$; $R_{w2} = 0.093$
Goodness-of-fit	$S = 1.17$ [$F_o > 4\sigma(F_o)$]
Number of parameters	181
Extinction coefficient	0.013(2)
$(\Delta\rho)_{max,\ min}$/e Å^{-3}	1.012; −0885
W	$W = 1/[\sigma^2(F_o^2) + (0.050P)^2 + 0.94P]$
	$P = [\max(F_o^2, 0) + 2F_c^2]/3$

Table 2
Positional and thermal parameters for $Na_{1/2}Cu_{4/3}Fe_2(PO_4)_3$

Atom	Occupancy	x	y	Z	U
Na	1	0	$\frac{1}{2}$	$\frac{1}{2}$	0.059(2)
(Cu, □)	0.66	$\frac{1}{2}$	$\frac{1}{2}$	$\frac{1}{2}$	0.0175(2)
Cu	1	0.7657(1)	0.3032(1)	0.7787(1)	0.0066(2)
Fe(1)	1	0.5445(1)	0.2184 (1)	0.0274(1)	0.0122(2)
Fe(2)	1	0.1191(1)	0.0485(1)	0.3845(1)	0.0063(2)
P(1)	1	0.0958(2)	0.2713(2)	0.1289(1)	0.0062(2)
O(11)	1	−0.1439(5)	0.2451(3)	0.0039(3)	0.0107(4)
O(12)	1	0.2508(4)	0.2190(3)	0.0338(3)	0.0127(4)
O(13)	1	0.0626(4)	0.1513(3)	0.2267(3)	0.0134(4)
O(14)	1	0.2061(4)	0.4676(3)	0.2492(3)	0.0132(4)
P(2)	1	0.6007(2)	0.0921(2)	0.3327(1)	0.0065(2)
O(21)	1	0.3798(4)	−0.0307(3)	0.3379(3)	0.0080(4)
O(22)	1	0.5742(4)	0.0488(3)	0.1542(3)	0.0084(4)
O(23)	1	0.8121(4)	0.0320(3)	0.4147(3)	0.0095(4)
O(24)	1	0.6365(4)	0.2868(3)	0.4203(3)	0.0152(4)
P(3)	1	0.2681(2)	0.3490(2)	0.7344(1)	0.0063(2)
O(31)	1	0.4808(4)	0.3055(3)	0.8374(3)	0.0090(4)
O(32)	1	0.0364(4)	0.2367(3)	0.7344(3)	0.0098(4)
O(33)	1	0.2620(4)	0.2992(3)	0.5604(3)	0.0106(4)
O(34)	1	0.2942(4)	0.5482(3)	0.8000(3)	0.0115(4)

2.3. Magnetic susceptibility

Magnetic susceptibility measurements were carried out with a Quantum Design SQUID MPMS-5S magnetometer. Data were recorded at a constant applied magnetic field of 0.5 T, in the temperature range 2–380 K.

2.4. Mössbauer spectroscopy

Room temperature Mössbauer measurements were performed with a constant acceleration HALDER-type spectrometer using a room temperature ^{57}Co source [Rh matrix] in the transmission geometry. The polycrystalline absorbers containing about 10 mg cm^{-2} of iron were used to avoid the experimental widening of the peaks. The velocity was calibrated using pure iron metal as the standard material.

3. Results and discussion

3.1. Structure description

As shown by Fig. 1, the $Na_{1/2}Cu_{4/3}Fe_2(PO_4)_3$ structure adopts a complex three-dimensional framework of FeO_6

Table 3
Main interatomic distances and angles in $Na_{1/2}Cu_{4/3}Fe_2(PO_4)_3$

Fe(1)	O(12)	O(34)	O(11)	O(22)	O(31)	O(22)′			
O(12)	1.879(3)	2.783(4)	2.463(4)	2.789(4)	2.828(4)	3.009(5)			
O(34)	93.4(2)	1.941(3)	2.463(4)	3.062(4)	2.517(4)	4.086(5)			
O(11)	172.18(2)	83.9(2)	2.009(3)	2..875(4)	2.630(4)	3.028(4)			
O(22)	90,8(2)	100.5(2)	96.9(2)	2.037(3)	2.826(4)	2.574(4)			
O(31)	92.3(2)	98.8(2)	80.9(2)	160.2(2)	2.041(3)	4.017(5)			
O(22)′	96.9(2)	169.7(2)	87.1(2)	75.7(2)	84.6(1)	2.161(3)			
Fe(2)	O(13)	O(21)	O(23)	O(33)	O(23)′	O(32)			
O(13)	1.857(3)	2.818(5)	2.899(4)	2.781(4)	3.947(5)	3.201(5)			
O(21)	94.3(2)	1.990(3)	2.501(4)	3.25(2)	2.907(4)	2.580(4)			
O(23)	97.0(2)	159.2(2)	2.014(3)	2.530(4)	2.856(4)	2.731(4)			
O(33)	91.0(2)	107.6(2)	89.7(2)	2.040(3)	2.856(4)	2.530(4)			
O(23)′	172.0(2)	80.6(2)	80.6(2)	81.4(2)	2.100(3)	2.737(4)			
O(32)	106.7(2)	77.5(2)	82.5(2)	161.4(2)	80.7(2)	2.128(3)			
M	O(24)	O(24)′	O(33)	O(33)′	O(14)	O(14)′			
O(24)	2.120(3)	4.240(5)	3.014(5)	3.210(5)	2.909(4)	3.499(5)			
O(24)′	180.0(1)	2.120(3)	3.210(5)	3.014(5)	3.499(5)	3.501(4)			
O(33)	93.5(1)	86.5(1)	2.280(3)	4.560(5)	3.165(4)	3.483(5)			
O(33)′	86.5(1)	93.5(1)	180.0(2)	2.280(3)	3.483(5)	3.165(4)			
O(14)	79.4(1)	100.6(1)	84.5(1)	95.5(1)	2.423(3)	4.829(5)			
O(14)′	100.6(1)	79.4(1)	95.5(1)	84.5(1)	180.0(1)	2.423(3)			
Cu	O(14)	O(32)	O(31)	O(21)	O(11)				
O(14)	1.913(3)	3.061(4)	2.860(4)	3.749(4)	2.546(4)				
O(32)	103.0(2)	2.001(3)	2.554(4)	2.580(4)	3.042(4)				
O(31)	93.1(2)	163.9(2)	2.023(3)	2.822(4)	2.630(4)				
O(21)	143.6(2)	79.5(2)	88.2(2)	2.034(3)	2.919(4)				
O(11)	128.9(2)	92.2(2)	76.6(2)	86.7(2)	2.211(3)				
P(1)	O(11)	O(12)	O(13)	O(14)	P(2)	O(21)	O(22)	O(23)	O(24)
O(11)	1.540(3)	2.436(4)	2.496(4)	2.546(4)	O(21)	1.558(4)	2.520(4)	2.501(4)	2.504(5)
O(12)	107.5(2)	1.515(3)	2.504(4)	2.522(4)	O(22)	108.3(2)	1.554(4)	2.502(4)	2.552(4)
O(13)	109.0(2)	111.1(2)	1.525(3)	2.456(5)	O(23)	106.6(2)	106.9(2)	1.561(3)	2.512(5)
O(14)	111.7(2)	111.2(3)	106.4(2)	1.538(3)	O(24)	110.5(2)	113.7(2)	110.6(2)	1.491(3)
P(3)	O(31)	O(32)	O(33)	O(34)	Na–O(32) × 2	2.579(2)			
O(31)	1.562(3)	2.554(4)	2.522(4)	2.517(4)	Na–O(31) × 2	2.731(2)			
O(32)	110.2(2)	1.553(3)	2.530(4)	2.496(4)	Na–O(24) × 2	2.969(2)			
O(33)	108.4(2)	109.6(2)	1.549(3)	2.481(4)	Na–O(11) × 2	2.339(2)			
O(34)	110.4(2)	109.4(2)	108.8(2)	1.506(3)					

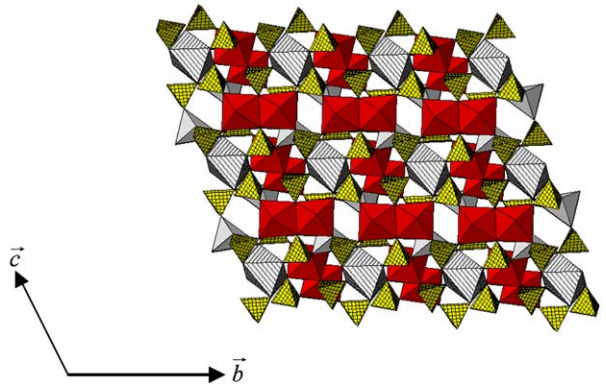

Fig. 1. A polyhedral view of framework as projected in the (b, c) plane. FeO_6 and $M(3)O_5$ are represented by dark and clear solid polyhedra, respectively. $M(1)O_6$ and PO_4 are filled by lined and dotted patterns, respectively.

and MO_6 ($M = Cu$, □) octahedra and CuO_5 trigonal bipyramids linked together via the phosphate tetrahedral.

The iron atoms occupy two distinct octahedral sites. Each of the $Fe(1)O_6$ and $Fe(2)O_6$ octahedra share opposite edges, with one equivalent FeO_6 octahedron and one CuO_5 trigonal bipyramid giving rise to zigzag chains that run along the [001] direction (Fig. 2). These chains, with a repeating sequence of –Fe(1)–Fe(1)–Cu–Fe(2)–Fe(2)– are connected to each other by the MO_6 octahedra through common corners. The framework constructed in this way contains large cavities of Na^+ occupation.

The polyhedral environments around $Fe(1)O_6$ and $Fe(2)O_6$ are depicted separately in Fig. 3. $Fe(1)O_6$ shares all of its corners with PO_4 tetrahedra. It is also connected to one CuO_5 bipyramid and to itself through common edges and thus four of its O atoms are three-bonded. The

$Fe(2)O_6$ exhibits a similar environment with one small difference being one supplementary three-bonded O atom. This later is shared with the MO_6 octahedron.

The similarity between the $Fe(1)O_6$ and $Fe(2)O_6$ neighborhoods induces a similarity of their geometries as indicated by their identical values (3.4%) determined for the deviation of individual bond lengths from their mean value BLD [12].

The connexion mode between the MO_6 octahedron and the other polyhedra is rather complex. This octahedron is connected through all its corners to the PO_4 tetrahedra. Four of the corners being also shared with two CuO_5 bipyramids and two $Fe(2)O_6$ octahedra, respectively. The M–O bond lengths range from 2.120(3) to 2.423(3) Å. The corresponding mean value of 2.273 Å is similar to that 2.284 Å observed in $Cu_3(PO_4)_2$ for the Cu^{2+} ion with C. $N = 6$ [13]. The corresponding BLD parameter (4.4%) is characteristic of a highly distorted octahedron.

The CuO_5 polyhedron shares its five O atoms with five PO_4 groups. Moreover, it is linked to the $Fe(1)O_6$ and $Fe(2)O_6$ octahedra by edge-sharing. The Cu–O bonds are very different with one very short, three intermediate and one very long.

The phosphate tetrahedra have P–O distances ranging from 1.491(3) to 1.562(3) Å. The averages ⟨P–O⟩ distances for P(1), P(2) and P(3) polyhedra are, respectively, 1.530 (2), 1.541 and 1.544 Å. Their overall average, 1.538 Å is in good agreement with those usually observed in anhydrous monophosphates.

The sodium ions occupy one crystallographically unique site. Their environment is very irregular. Assuming Na–O distances below 3.0 Å, this environment consists of eight oxygen atoms at four Na–O distances between 2.334(3) and 2.968(3) Å. The relatively high value calculated for the equivalent isotropic displacement parameter, ($U_{eq} = 0.06$) can be attributed to the partial occupancy of this site. The particularly high value of the anisotropic U_{33} parameter (0.11(4)) reveals a strong deformation of Na thermal ellipsoid in the [001] direction along which the tunnels that contain the sodium ins are oriented.

The structural data for $Na_{1/2}Cu_{4/3}Fe_2(PO_4)_3$ are consistent with those reported for the mineral Howardevansite $NaCuFe_2(VO_4)_3$ [9]. However, the title compound is featured by two main differences:

- the mutual presence of Fe^{3+} and Fe^{2+} ions while the $NaCuFe_2(VO_4)_3$ structure contains Fe^{3+} ions, exclusively,
- the partial occupancy, by Cu^{2+} ions of the M sites. These sites being totally occupied by Na^+ in NaCu $Fe_2(VO_4)_3$.

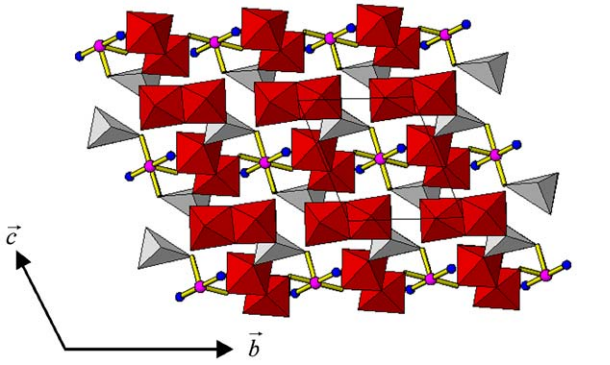

Fig. 2. A view of the infinite chains of edge sharing FeO_6 and $M(3)O_5$ polyhedra running along the $1\,0\,-\,1$ direction and connected through the $M(1)O_6$ octahedra.

3.2. Magnetic susceptibility

Fig. 4 shows the temperature dependence of the inverse magnetic susceptibility χ^{-1} for $Na_{1/2}Cu_{4/3}Fe_2(PO_4)_3$ at

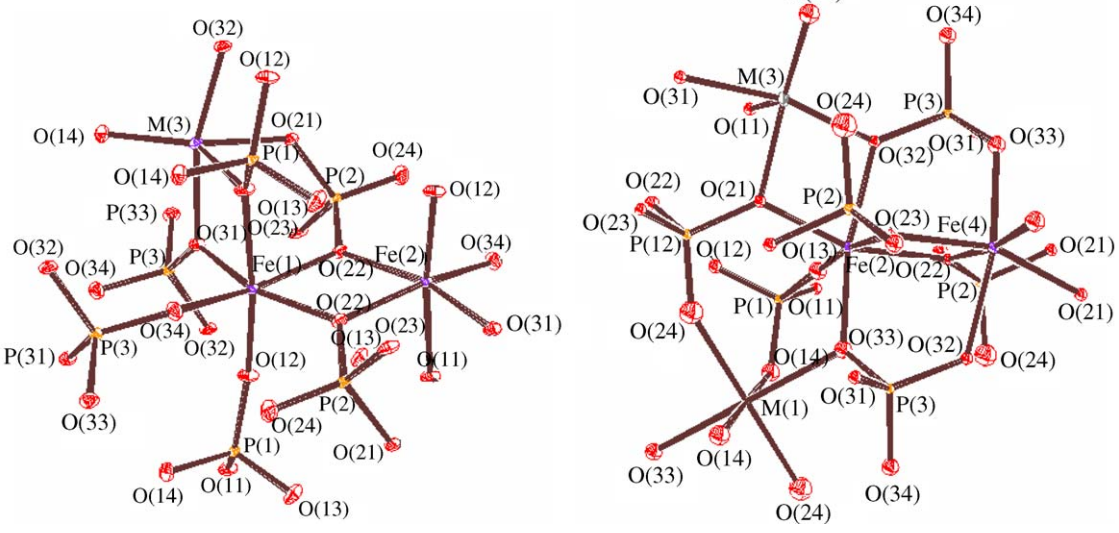

Fig. 3. The polyhedral environments around the $Fe(1)O_6$ and $Fe(2)O_6$ octahedra.

(2–280 K) temperature range. The analysis of the data indicates that the compound has an antiferromagnetic behavior with a Neel temperature of $T_N = 40$ K and a Curie constant per formula unit $C = 9.20$ emu K mol^{-1} in agreement with the spin only values and a ratio $Fe^{3+}/Fe^{2+} \approx 10.8\%$ corresponding to the formula $Na_{1/2}Cu_{4/3}Fe^{3+}_{1.83}Fe^{2+}_{0.17}(PO_4)_3$. The negative value of paramagnetic Curie temperature ($\theta = -89.3$ K) indicates that the dominant magnetic interactions accruing at low temperatures are antiferromagnetic and rather intense.

3.3. Mössbauer spectroscopy

The room temperature Mössbauer spectrum of $Na_{1/2}Cu_{4/3}Fe_2(PO_4)_3$ is shown in Fig. 5. The points represent experimental results, and the refined data are shown as solid lines. A preliminary refinement using Lorentzian profile lines shown that the spectrum consists of two doublets assigned to Fe^{2+} and Fe^{3+} ions, respectively. Nevertheless, the large values of the line width implied the existence of distributions of quadrupolar splittings and therefore of local iron environment. The best result was obtained using two distributions DIS(1) and DIS(2) for Fe^{3+} and one distribution DIS(3) for Fe^{2+}. The line width value was fixed at 0.25 mm s^{-1} for DIS(1) and DIS(2) and at 0.28 mm s^{-1} for DIS(3). The hyperfine parameters obtained from this refinement are given in Table 4. The isomer shifts For DIS(1) ($\delta_1 = 0.42$ mm s^{-1}) and DIS(2) ($\delta_2 = 0.46$ mm s^{-1}) are typical of Fe^{3+} ions in an octahedral environment. That of DIS(3) ($\delta_3 = 1.30$ mm s^{-1}) is consistent with Fe^{2+} ions with C. N. = 6. These results are in accordance with structural refinement which indicted the presence of a disordered distribution of Fe^{3+} and Fe^{2+} in two distinct sites with octahedral environments.

The profile of DIS(1) and DIS(2) (Fig. 6) seems to be nearly the same as it can be deduced from a comparison of

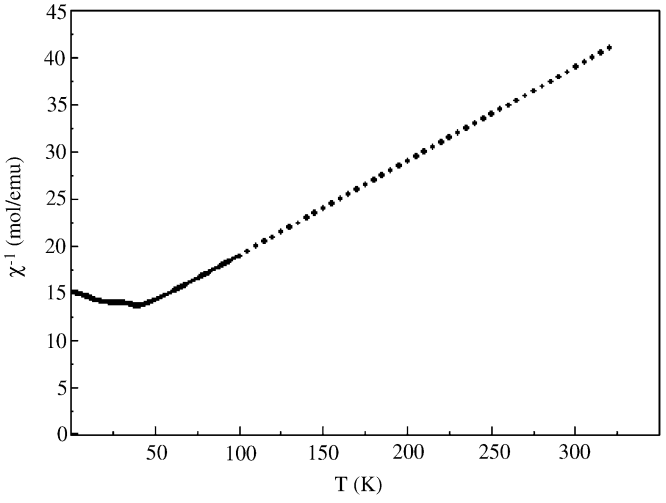

Fig. 4. A plot of the reciprocal susceptibility versus temperature for $Na_{1/2}Cu_{4/3}Fe_2(PO_4)_3$.

Table 4
Room temperature Mössbauer parameters

DIS	δ (mm s^{-1})	Γ_I (mm s^{-1})	Δ^a (mm s^{-1})	%^{a}
DIS1	0.42	0.25	1.10(1)	41(2)
DIS2	0.46	0.25	0.96(1)	44(2)
DIS3	1.30	0.25	2.54(3)	15(2)

[a]Parameters refined.

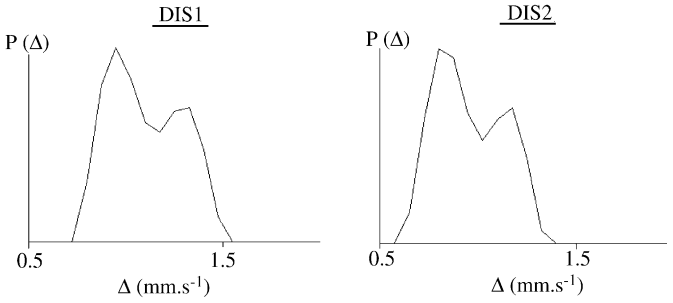

Fig. 6. Distributions of quadrupolar splittings.

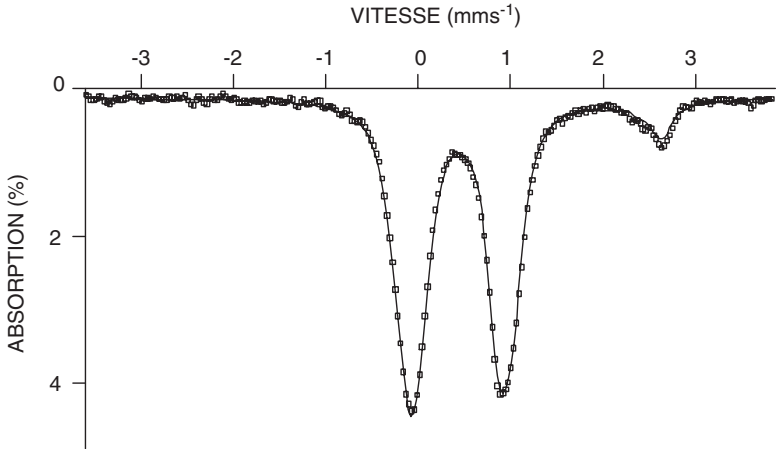

Fig. 5. Mössbauer spectrum for $Na_{1/2}Cu_{4/3}Fe_2(PO_4)_3$ at room temperature.

their average quadrupolar splittings ($\langle \Delta_1 \rangle = 1.10\,\mathrm{mm\,s^{-1}}$; $\langle \Delta_2 \rangle = 0.96\,\mathrm{mm\,s^{-1}}$). Moreover, the populations of Fe^{3+} and Fe^{2+} (85% and 15%, respectively) correspond to those predicted by the X-ray diffraction and the magnetic susceptibility studies.

References

[1] B. Lajmi, M. Hidouri, M. Rzeigui, M.B. Aamara, Mater. Res. Bull. 37 (15) (2002) 2407.
[2] M. Hidouri, B. Lajmi, M.B. Amara, Acta Crystallogr. C 58 (2002) i147.
[3] B. Lajmi, M. Hidouri, M.B. Aamara, Acta Crystallogr. C 58 (2002) i156.
[4] M. Hidouri, B. Lajmi, A. Driss, M.B. Amara, Acta Crystallogr. E 59 (2003) i7.
[5] M. Hidouri, B. Lajmi, A. Wattiaux, L. Fournes, J. Darriet, M.B. Amara, J. Alloys Comp. 358 (2003) 36.
[6] B. Lajmi, M. Hidouri, A. Wattiaux, L. Fournes, J. Darriet, M.B. Amara, J. Alloys Comp. 361 (2003) 77.
[7] M. Hidouri, B. Lajmi, A. Wattiaux, L. Fournes, J. Darriet, M.B. Amara, J. Solid State Chem. 177 (2004) 55.
[8] M. Hidouri, B. Lajmi, A. Driss, M.B. Amara, J. Chem. Crystallogr. 34 (2004) 769.
[9] J.M. Hughes, J.W. Drexler, C.F. Campana, M.L. Malinconico, Am. Mineral. 73 (1988) 181.
[10] A. Altomare, G. Cascarano, C. Giacovazzo, A. Guagliardi, J. Appl. Crystallogr. 26 (1993) 343.
[11] G.M. Sheldrick, Institüt für Anorganische Chemie der Universität Tammanstrasse 4, D3400 Göttinguen, Germany, 1998.
[12] K. Robinson, G.V. Gibbs, P.H. Ribbes, Science 172 (1971) 567.
[13] G.L. Shoemaker, J.B. Anderson, E. Kostiner, Acta Crystallogr. B 33 (1977) 2969.